Digital image analysis of EUS images accurately differentiates pancreatic cancer from chronic pancreatitis and normal tissue

Ananya Das, MD, FASGE, Cuong C. Nguyen, MD, Feng Li, MD, Baoxin Li, PhD

Scottsdale, Arizona, USA

Background: Concomitant changes of chronic pancreatitis markedly degrade the performance of EUS in diagnosing pancreatic adenocarcinoma (PC). Digital image analysis (DIA) of the spatial distribution of pixels in a US image has been used as an effective approach to tissue characterization.

Objective: We applied the techniques of DIA to EUS images of the pancreas to develop a classification model capable of differentiating pancreatic adenocarcinoma from non-neoplastic tissue.

Design: Representative regions of interest were digitally selected in EUS images of 3 groups of patients with normal pancreas (group I), chronic pancreatitis (group II), and pancreatic adenocarcinoma (group III). Texture analyses were then performed by using image analysis software. Principal component analysis (PCA) was used for data reduction, and, later, a neural-network–based predictive model was built, trained, and validated.

Setting: Tertiary academic medical center.

Patients: Patients undergoing EUS of the pancreas.

Results: A total of 110, 99, and 110 regions of interest in groups I, II, III, respectively, were available for analysis. For each region, a total of 256 statistical parameters were extracted. Eleven parameters were subsequently retained by PCA. A neural network model was built, trained by using these parameters as input variables for prediction of PC, and then validated in the remainder of the data set. This model was very accurate in classifying PC with an area under the receiver operating characteristic curve of 0.93.

Limitation: Exploratory study with a small number of patients.

Conclusions: DIA of EUS images is accurate in differentiating PC from chronic inflammation and normal tissue. With the potential availability of real-time application, DIA can develop into a useful clinical diagnostic tool in pancreatic diseases and in certain situations may obviate EUS-guided FNA. (Gastrointest Endosc 2008;67:861-7.)

Nearly a quarter of patients who undergo EUS for focal pancreatic lesions, which are clinically suspicious of being neoplastic in nature, have features of underlying chronic pancreatitis (CP).[1,2] Several recent studies showed that the diagnostic yields of EUS and EUS-guided FNA are markedly decreased in the presence of CP because both neoplastic and inflammatory changes usually have a similar appearance as assessed subjectively even by experienced endosonographers.[1-3] Because the yield of EUS-guided FNA is heavily dependent on accurate targeting of the area of interest based on the interpretation of EUS images, false-negative rates of EUS-guided FNA are often unacceptably high in some clinical settings. Two-dimensional digital images, such as EUS images, are composed of pixels, which are basic finite elements of a digital image; the arrangement of these pixels reflects the structure and texture of the object that has been imaged. Digital image analysis (DIA) computes relevant mathematical and statistical parameters based on the distribution of these pixels in a digital image. It is known that the presence of pathology (such as inflammatory and neoplastic changes) alters the tissue architecture. These architectural changes, unfortunately, are often beyond the perceptive ability of visual interpretation. The changes, however, are subtly reflected in digital images of the tissue.[4] DIA techniques have been widely used in the field of biomedical imaging

Abbreviations: ANN, artificial neural network; CP, chronic pancreatitis; DIA, digital image analysis; MPD, main pancreatic duct; PC, pancreatic adenocarcinoma; PCA, principal component analysis; ROC, receiver operating characteristic curve; ROI, region of interest.

0016-5107/$32.00
doi:10.1016/j.gie.2007.08.036

(including US and echocardiography) for differentiation and characterization of different pathologic lesions and also for studying tissue structure and function.[4,5] Initial reports of the application of this technique in the area of EUS are very encouraging,[6,7] and there is increasing interest in EUS for virtual (optical) biopsy when using different emerging technologies.[8] In the current study, we systematically applied the techniques of DIA to EUS images obtained during an EUS examination of the pancreas to develop a classification model capable of differentiating pancreatic adenocarcinoma (PC) from non-neoplastic pancreatic tissue.

Capsule Summary

What is already known on this topic

- Chronic pancreatitis decreases the reliability of EUS in diagnosing pancreatic cancer.
- Digital image analysis of US amplitude is an effective approach to tissue characterization.

What this study adds to our knowledge

- Digital image analysis of EUS images was accurate in differentiating pancreatic cancer from chronic inflammation and normal tissue.

PATIENTS AND METHODS

Patients

A review of the endoscopic database in our institution was performed to identify patients with a normal EUS examination of the pancreas (n = 22; group I), patients with CP (n = 12; group II), and patients with PC (n = 22; group III). Patients with a normal pancreas underwent EUS for indications unrelated to the pancreas. All patients with PC had their diagnosis established by EUS-guided FNA. Patients with CP were diagnosed on the basis of their clinical presentation and at least two different imaging modalities (ie, CT, MRCP, or ERCP) that showed the characteristic features of CP, in addition to EUS findings of CP. As reported in published literature, there are distinct EUS features of CP, and, in our study, we required the presence of 5 or more of the following features for the EUS diagnosis of CP (ie, echogenic strands, echogenic foci, lobularity, cystic changes, main pancreatic duct (MPD) irregularity, hyperechoic MPD, MPD dilation, visible side branches, and stones).[9,10] The study was approved by the institutional review board, and the requirement for informed consent was waived because only de-identified patient data were used for this study.

Acquisition of EUS images

All EUS examinations were done by two experienced endosonographers (A.D., C.N.) by using a mechanical scanning radial array echoendoscope (GF-UM ultrasonic gastrovideoscope; Olympus America Inc, Centerville, Pa) at 7.5 MHz frequency. The entire EUS examination was digitally recorded by using a digital video recorder in the DVD recorder file (.VRO) format; the salient findings were recorded as still images by using the freeze button on the echoendoscope. The digital video recordings were later reviewed, and the highest-quality still images were digitally captured and saved as digital files in the Windows bitmap (.BMP) format for further analysis, which was performed on a standard desktop computer. The sequential steps used in this study for DIA of EUS images are shown in Figure 1.

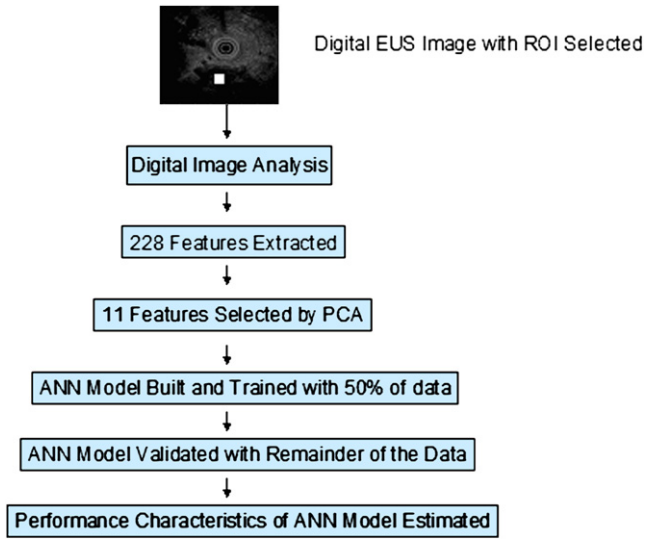

Figure 1. Summary of a flow diagram of the steps of DIA, selection by PCA, and training and validation of the ANN model.

Image analysis

Multiple, small, approximately 15 × 15-pixel blocks were digitally selected on the images to identify regions of interest (ROIs) in the representative areas of the images that corresponded to the most abnormal areas in those patients with PC or CP. In patients with CP, we selected ROIs that focused on the parenchymal features of CP and chose the ROIs from areas that had the highest concentration of parenchymal features of echogenic foci and strands and lobularity. If focal changes of CP or mass-like lesions were present, then these areas were selectively chosen. In patients with a focal pancreatic mass, the most hypoechoic areas, particularly in relationship with a ductal stricture (if present but actually avoiding the dilated ducts), were evaluated. In patients with normal pancreas, the ROIs were selected from the head and body of the pancreas, away from the main pancreatic duct. While selecting the ROIs, the reviewing endosonographer was not blinded to the final diagnosis. Also, careful

attention was given to avoid selecting any ROIs that would be composed entirely of an anechoic area or the edges of an image, which are known to give erroneous results on DIA.[11] The Image J (1.36 b version; available at http://rsb.info.nih.gov/ij/), a user-friendly Java image analysis software available in the public domain, was used for image analysis. When using this software, texture analysis was performed to extract texture parameters for each ROI.[5] A digital image is composed of rectangular blocks or pixels (picture elements), and each pixel is represented by a set of coordinates and a value that represents the gray-level intensity of that picture element in space. In digital images, the allowed gray-level values that a pixel may assume are limited. The gray-level values consist of integer numbers that range from 0 to 2b-1; b stands for the number of bits of the image, 0 generally represents black, and white is represented by 255 (in an 8-bits image). The texture analysis of digital images is, in principle, a technique for evaluating the distribution and the spatial variation of the pixel intensities.

The following texture parameters were extracted: histogram, absolute gradient, run-length matrix, co-occurrence matrix, model vector parameters of an autoregressive model, and wavelet energy parameters.[4,5] The histogram of an image is the count of how many pixels in the image possess a given gray-level value. Many parameters, such as the mean, variance, and percentiles, of the histogram may be derived. The mean of the histogram provides the mean gray-level value of the image. A percentile gives the highest gray-level value under which a given percentage of the pixels in the image are contained.

The absolute gradient of an image measures the spatial variation of gray-level values across the image. Thus, if, at a point in the image, the gray level varies abruptly from black to white, we have a high-gradient value at that point; whereas, if it varies smoothly from a dark gray to a slightly lighter gray, we have a low-gradient value at that point. The gradient may be positive or negative, depending on whether the gray level varies from dark to light or from light to dark. However, because, in general, what is of interest is whether we have an abrupt or a smooth gray-level variation, the absolute gradient is used.

The run-length matrix is a way of searching the image, always across a given direction, for runs of pixels that have the same gray-level value. Many different run-length matrices may be computed for a single image, one for each chosen direction. In practice, normally, 4 matrices are computed: the horizontal, vertical, and two diagonal directions. The fraction of image in runs is a measure of the percentage of image pixels that are part of any of the runs considered for the matrix computing, and the short-run emphasis is a measure of the proportion of runs that occur in the image that has a short length.

The co-occurrence matrix is a technique that allows for the extraction of statistical information from the image regarding the distribution of pairs of pixels. It is computed by defining a direction and a distance, and pairs of pixels separated by this distance, computed across the defined direction, are analyzed. A count is then made of the number of pairs of pixels that possess a given distribution of gray-level values. Each entry of the matrix thus corresponds to one such gray-level distribution. As in the case of the run-length matrix, there may be many co-occurrence matrices computed for a single image, one for each pair of distances and directions defined. Examples of parameters computed from the co-occurrence matrix are the contrast and the entropy. The contrast of an image refers to how much difference, or definition, there is between gray-level values of different objects in the image. The entropy measures the randomness or the homogeneity of the pixel distribution, which is a measure of the degree of disorder in the image. The run-length matrix-based parameters were computed 4 times for each ROI (for vertical, horizontal, 45°, and 135° directions). The co-occurrence matrix-based parameters were computed up to 20 times, for (d,0), (0,d), (d, d), (d, −d), in which the distance d can take values of 1, 2, 3, 4, and 5.

The autoregressive model assumes a local interaction between image pixels in that the pixel gray-level value is a weighted sum of the gray-level values of the neighboring pixels. Expressed differently, it is a way of describing shapes within the image, by finding relations between groups of neighboring pixels. If the gray-level value of a two-dimensional image varies fast, that is, if there are many variations within a small piece of the image, then we associate a high spatial frequency to this part of the image. In turn, if the gray level value varies slowly, then the region has a low spatial frequency.

Wavelets represent a technique that analyzes the frequency content of an image within different scales of that image. This analysis yields a set of wavelet coefficients that correspond to different scales and to different frequency directions. When computing the wavelet transform of an image, we associate to each pixel a set of numbers (the wavelet coefficients) that characterizes the frequency content of the image at that point over a set of scales. From these coefficients, we can compute texture parameters.[4,5]

Feature selection by principal component analysis

Because of the large number of features extracted (with 228 texture parameters extracted from each ROI) and, also, because many of these parameters are likely to be correlated with each other, the technique of principal component analysis (PCA) was used to reduce the dimensionality (number of variables) to provide compact data sets but at the same time retain as much of the information (variation) as possible. PCA is one of the commonly used methods for data reduction to remove redundant (highly correlated) variables from a large data set.[12] We performed the PCA for data reduction by using statistical

software (SPSS 11.0 for Windows; SPSS Inc, Chicago, Ill). We used a variance maximizing (varimax) rotational strategy to maximize the variance of the newly extracted feature while minimizing the variance around the extracted feature. To decide how much data reduction should be done or how many features to extract, we used both the Kaiser criterion based on eigenvalues and the Scree test. In the Kaiser criterion, eigenvalues of more than one were retained, meaning that unless a feature extracts at least as much as the equivalent of one original variable, it would be dropped. In the Scree test, the eigenvalues for successive factors are displayed in a simple line plot, and the point where the smooth decrease of eigenvalues appears to level off to the right of the plot is noted to determine the number of appropriate features.[11] Once the PCA was performed, we used the rotated component matrix to understand what the extracted features represented. Examining the correlation of the original variables with a particular extracted feature allowed us to understand what that particular extracted feature mostly represented and to what extent (by examination of the component's score coefficient that is a numerical measure of the degree of correlation). We also examined the correlation matrix of the individual component scores of the extracted features to make sure that there was no significant correlation among them; by definition, there should not be any linear correlation among the extracted features.

Artificial neural network

Artificial neural network (ANN) models are by far the most robust of all available classification techniques; because of their ability to model the complex nonlinear multidimensional interactions inherent in image analysis algorithms, ANN-based models have traditionally been used in DIA. An ANN model was built by using neural-network software (Statistica Neural Networks 4.0; Statsoft Inc, Tulsa, Okla), as described earlier.[13-15] Briefly, an initial network was constructed by using half of the data set (selected randomly), with features selected by PCA as input variables, and the single output variable was a dichotomy (presence/absence) of PC. During training, the outcome variable was made known to the network so that the predicted output of the network could be compared with the actual result and, in case of errors, the network was retrained by back propagation. Different types of networks (multilayered perceptron, radial basis function, and probabilistic and generalized regression neural networks) were tested, and the best network and architecture were retained.[13] The problem of overfitting or overlearning was encountered by using cross-verification during training. The performance of the algorithm was dynamically monitored during training, and several training algorithm parameters, such as the number of epochs, the learning rate, the momentum, and the stopping conditions for the training algorithm, were continually adjusted to reduce overlearning. By a process of repeated heuristic experimentation, these parameters were tested, and the ones that provided the best results were retained. The algorithm for training by back propagation was detailed elsewhere.[13,15] Data from the remaining 50% of the ROIs were used for validation of the neural networks. During validation, the actual pathology (absence or presence of PC) was concealed from the network, and the predictive accuracy of the output of the neural network was compared with the actual pathology.

Evaluation of the performance of the neural network

In the validation model, the sensitivity, specificity, positive-predictive value, negative-predictive value, and likelihood ratios for positive and negative tests of the ANN model were calculated. Also, the area under the receiver operating characteristic curve (ROC) for the ANN for prediction of correct pathology (presence or absence of cancer) was calculated.

RESULTS

A total of 110, 99, and 110 ROIs in groups I, II, and III, respectively, were available for analysis. For each ROI, a total of 228 parameters were extracted by the image analysis software in the histogram, absolute gradient, run-length matrix, co-occurrence matrix, autoregressive model, and wavelet analysis categories. PCA performed for data reduction extracted 11 features that cumulatively explained 96% of the variability in the original 228 variables. The scree plot shows the first 11 features in the steep part of the slope that explained the majority of the variability represented by the original variables (Figs. 1 and 2).

Examination of the rotational component matrix of the PCA allowed understanding of what the extracted features represented. Six of the 11 extracted by PCA were derived from co-occurrence matrix parameters (ie, angular second momentum, sum of squares, correlation, entropy, inverse difference momentum, and difference variance) and represented approximately 85% of the total variability. Two other extracted features correlated best with wavelet-analysis–based parameters and explained 7% more of the total variability. One feature each correlated the most with gradient-based (ie, kurtosis of absolute gradient), run-length–based (ie, gray-level nonuniformity), and first-order histogram–based parameters (ie, kurtosis). Evaluation of the correlation matrix of the individual component scores of the 11 extracted features showed no significant correlation among them (Fig. 3).

The neural network model that was trained and validated by using the extracted 11 features from all the ROIs was a multilayered perceptron neural network, with 9 final inputs and 8 hidden layers, and was very

accurate in classifying ROIs belonging to group III. In the validation set of 159 ROIs in which the network was blinded to the actual diagnosis, the ANN model was very sensitive (93%, 95% CI, 89%-97%) and specific (92%, 95% CI, 88%-96%), with excellent positive (87%, 95% CI, 82%-92%) and negative (96%, 95% CI, 93%-99%) predictive values. The area under the ROC was 0.93. Thus, the neural network model built with the 11 features extracted by PCA from the parameters derived by image analysis was very powerful in identifying ROIs that represented PC on EUS images. To evaluate the performance characteristics of the model in differentiating ROIs selected from normal pancreas and those from CP, we also applied the trained ANN model to the validation set after ignoring ROIs that represent PC. The model was 100% accurate with 100% sensitivity and specificity in accurately classifying areas of normal pancreas from CP.

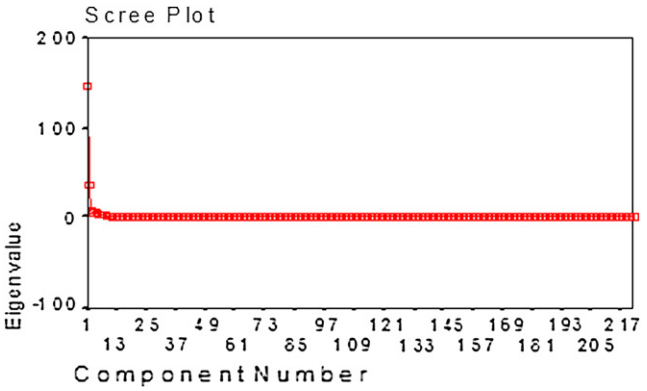

Figure 2. The scree-plot derived from the PCA shows that the first 11 features in the steep part of the slope explain the majority of the variability represented by the original 228 variables.

DISCUSSION

Image analysis is the extraction of meaningful information from images and can be as simple as reading bar-coded tags or as sophisticated as automated face recognition and remote sensing. With the ubiquitous use of digital photography and the expanding availability of powerful microprocessors at low cost, image analytic techniques are being applied to a wide spectrum of scientific and industrial disciplines, which range from medicine, astronomy, defense, security, manufacturing, document processing, to robotics and artificial intelligence. Although computers are indispensable for the analysis of large amounts of data involved in any image analytic technique, the human visual cortex remains the most complex image analysis tool, and, thus, it is no surprise that ANNs that are inspired by human perception models are an integral part of most image analytic tools. Image analysis has already made a huge impact in the field of biomedical imaging (eg, magnetic resonance imaging and positron emission tomography). It, however, is surprising that, in the field of GI endoscopy, which is primarily involved with image acquisition and interpretation, there is a paucity of published information on the application of techniques of image analysis. In the current study, we applied techniques of image analysis and neural networks to develop a model for the accurate identification of areas of PC in EUS images. For diagnosis of PC, EUS is a widely used imaging modality. It is well accepted that, in the presence of changes from CP, which are not uncommon in patients with PC, EUS is not able to definitively and reliably differentiate neoplastic changes from those of chronic inflammation. Published studies reported that even with the application of EUS-guided FNA, the sensitivity to diagnose PC in the setting of CP may be reduced by as much as 45%. In addition, interpretation of EUS images is inherently subjective and dependent on the endosongrapher's experience.[1,2] In the present study, the accuracy of the trained ANN model based on the DIA of EUS images was 100% accurate in differentiating CP from normal pancreas, which was not surprising given that all patients with CP in our study had at least moderately severe changes of CP on EUS imaging. More importantly, the performance characteristics of this model in differentiating CP from PC closely rivaled that of EUS-guided FNA, which may be considered the current benchmark in the relatively noninvasive diagnosis of PC. Our model has a very high negative predictive value, which may be more important from a clinical perspective in many patients with a focal pancreatic lesion but with a low clinical suspicion of PC. It should be noted that, with a decreased prevalence of a disease, the negative predictive value of a test generally increases. In our selected sample, approximately a third of ROIs represented PC, which is much higher than would be expected in an unselected population of patients with CP with focal lesions. Thus, one can argue that if DIA is used in an unselected sample of CP undergoing EUS for evaluation of focal lesions with an expected prevalence of PC lower than the current study, then its already attractive negative predictive value is expected to be maintained if not increased.

Although the theoretical basis of image analysis and parameter extraction from gray-level sonographic images is very well founded, and several algorithms based on computer-aided extraction and pattern recognition of these features have been reported, there are only a few reports of image analytic techniques applied to EUS. In a recent study, Loren et al[6] reported the feasibility of computer-assisted analysis of images of mediastinal lymph nodes in patients with esophageal cancer for identification of malignant lymph nodes, although they did not attempt to develop a pattern recognition model. In a study similar to ours, Norton et al[7] reported the utility of neural network analysis of EUS images to differentiate between PC and CP by using 4 different image parameters. Although they reported a high sensitivity, the technique had only

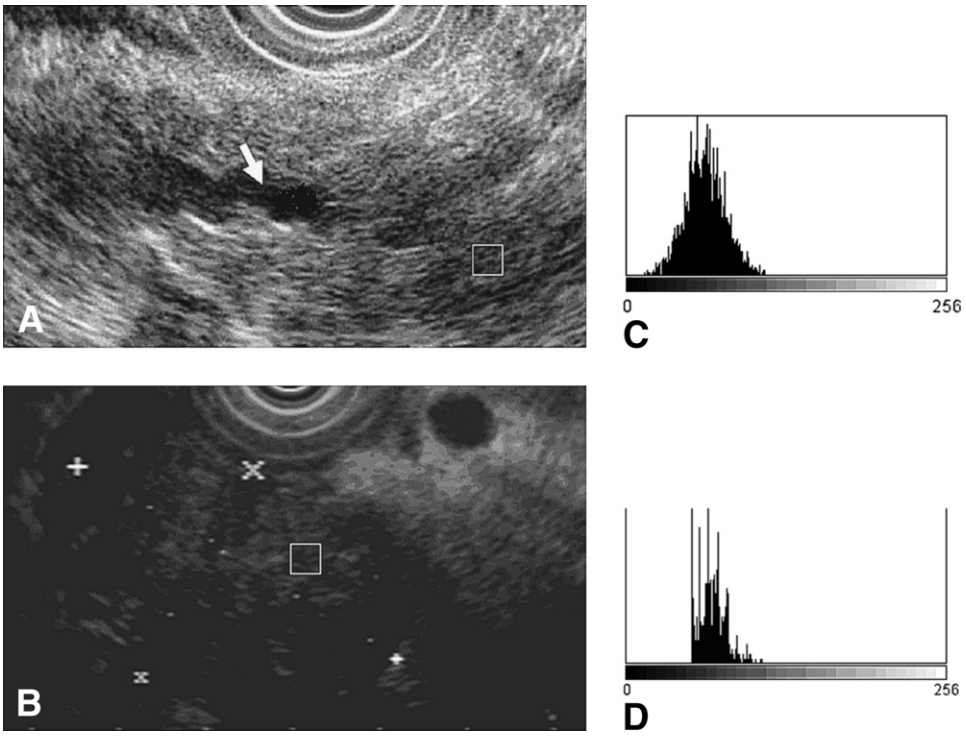

Figure 3. An example of the image analysis technique used in this study. **A**, The EUS images of changes consistent with CP (*arrow* showing a dilated irregular pancreatic duct) in a patient. **B**, The EUS images of changes consistent with a pancreatic mass confirmed to be an adenocarcinoma in another patient. **C**, Histogram of a region of interest in each image (marked with *rectangles*) in patient in Figure 3A. **D**, Histogram of a region of interest in each image (marked with *rectangles*) are shown in the patient in Figure 3B. Although the two regions of interest appear quite similar in the EUS images, the histograms are very different in the distribution of pixel gray-level values; the histogram was only one of the many texture parameters used in this study.

50% specificity. Overall, they concluded that this technique compared favorably with human interpretation and is a useful adjunct to EUS. The much improved outcomes of our study were the results of two factors. First, our analysis used a much larger number of image-texture parameters; up to 228 were incorporated into our classification model. Second, because of the publication of the earlier report by Norton et al,[7] image analysis, because of the continuing and robust advances in computer hardware, has evolved into a much more mature and powerful tool, enabling techniques such as autoregressive modeling and wavelet analysis. It, however, is interesting to note that, in both of these studies, some parameters, eg, gray-level nonuniformity (which analyzes images in terms of variance between gray scales of adjacent pixels), were common features in discriminating PC.

There are some limitations of our study. In our study, we used digital EUS images acquired by radial scanning echoendoscopes with fixed settings in terms of gain and contrast. The impact of using a different set of equipment and settings on our findings is unknown, and it will be important to validate our results with other commercially available EUS equipment and by other investigators. When selecting the ROIs, the reviewing endosonographer was not blinded to the final diagnosis; this may have biased the results of the analysis. In all patients with PC, the PC was confirmed by EUS-guided FNA, which is not the criterion standard for a diagnosis of PC. Also, the diagnosis of CP was based on clinical features and multiple imaging studies; histopathologic confirmation was not clinically indicated in these patients. In the current study, DIA was not performed in real time, and the practical utility of such a technique can only be convincing if it can be performed in real time. It should be pointed out that once the technique is established, it is very likely that a real-time application can be developed as add-on software. Most EUS processing modules currently have a built-in capability to perform basic but real-time image processing tasks at the touch of a button. The sample size and power calculation for both data-reduction techniques, eg, PCA, and also for classification techniques, eg, neural networks, are areas of considerable debate.[16,17] Although the overall number of patients in this exploratory analysis was small, we attempted to adhere to the basic principles of determining sample size for an acceptable analysis. For PCA, it is recommended that, to have an adequate sample size, the ratio of input variables per component or factor extracted by PCA should be between 15:1 and 30:1.[16] From the original 228 variables in this study, 11 features were extracted at a ratio of approximately 20:1, which satisfies the recommended criterion. Neural network predictions are thought to be reasonably accurate, even when the

sample size is relatively small. However, in constructing such a model, it is important to have a reasonable number of ''positive'' cases in the training set for optimization of training; a subject with an outcome of interest (in our study, a ROI representing PC) to input variables ratio of 3:1 to 6:1 is recommended.[17] In our analysis, which compared PC to non-PC cases, in the training set, a total of approximately 160 ROIs were used, with 11 input features and, of them, 52 ROIs were positive for cancer, thus providing a ratio of 4.8 per input feature. Thus, it appeared overall that, despite the small number of patients, the sample size in the current PCA-based and ANN-based analyses was adequate.

In conclusion, in this exploratory analysis, we report encouraging results with respect to the potential utility of a classification model based on DIA of EUS images in differentiating PC from non-neoplastic pancreatic tissue by using commercially available hardware and software for image analysis. Further enhancement (in terms of real-time application and, also, incorporation of a suitable ''red-flag'' or auto-detection technology) and confirmation and validation in larger studies will be needed before this technique can be recommended for incorporation in clinical practice.

DISCLOSURE

The authors report that there are no disclosures relevant to this publication. A. Das is the recipient of the 2006 Olympus Endoscopy Career development award awarded by the American Society for Gastrointestinal Endoscopy.

REFERENCES

1. Fritscher-Ravens A, Brand L, Knofel WT, et al. Comparison of endoscopic ultrasound-guided fine needle aspiration for focal pancreatic lesions in patients with normal parenchyma and chronic pancreatitis. Am J Gastroenterol 2002;97:2768-75.
2. Brand B, Pfaff T, Binmoeller KF, et al. Endoscopic ultrasound for differential diagnosis of focal pancreatic lesions, confirmed by surgery. Scand J Gastroenterol 2000;35:1221-8.
3. Varadarajulu S, Tamhane A, Eloubeidi MA. Yield of EUS-guided FNA of pancreatic masses in the presence or the absence of chronic pancreatitis. Gastrointest Endosc 2005;62:728-36.
4. Castellano G, Bonilha L, Li LM, et al. Texture analysis of medical imagesClin Radiol 2004;59:1061-9.
5. Robb RA. Biomedical imaging, visualization and analysis. New York: Wiley-Liss; 2000.
6. Loren DE, Seghal CM, Ginsberg GG, et al. Computer-assisted analysis of lymph nodes detected by EUS in patients with esophageal carcinoma. Gastrointest Endosc 2002;56:742-6.
7. Norton ID, Zheng Y, Wiersema MS, et al. Neural network analysis of EUS images to differentiate between pancreatic malignancy and pancreatitis. Gastrointest Endosc 2001;54:625-9.
8. Fritscher-Ravens A. Blue clouds and green clouds: virtual biopsy via EUS elastography? Endoscopy 2006;38:416-7.
9. Wallace MB, Hawes RH, Durkalski V, et al. The reliability of EUS for the diagnosis of chronic pancreatitis: interobserver agreement among experienced endosonographers. Gastrointest Endosc 2001;53:294-9.
10. Gleeson FC, Topazian M. Endoscopic retrograde cholangiopancreatography and endoscopic ultrasound for diagnosis of chronic pancreatitis. Curr Gastroenterol Rep 2007;9:123-9.
11. Image segmentation. In: Gonzalez RC, Woods RE, editors. Digital image processing. 2nd ed. Upper Saddle River (NJ): Prentice Hall; 2002. p. 585-95.
12. Joliffe IT, Morgan BT. Principal component analysis and exploratory factor analysis. Stat Methods Med Res 1992;1:69-95.
13. Haykin S. Neural networks: a comprehensive foundation. New York: McMillan Publishing; 1994.
14. Cross SS, Harrison RF, Kennedy RL. Introduction to neural networks. Lancet 1995;346:1075-9.
15. Das A, Ben-Menachem T, Cooper GS, et al. Prediction of outcome in acute lower gastrointestinal haemorrhage based on an artificial neural network: internal and external validation of a predictive model. Lancet 2003;362:1261-6.
16. Osborne JW, Costello AB. Sample size and subject to item ratio in principal components analysis. Practical Assessment. Research & Evaluation 2004;9:311-3.
17. Chan HP, Berkman S. Classifier design for computer-aided diagnosis: effects of finite sample size on the mean performance of classical and neural network classifiers. Med Phys 1999;26:2654-68.

Received January 18, 2007. Accepted August 20, 2007.

Current affiliations: Division of Gastroenterology and Hepatology (A.D., C.C.N., F.L.), Department of Internal Medicine, Mayo Clinic Arizona, Scottsdale, Department of Computer Science and Engineering (B.L.), Arizona State University, Phoenix, Arizona, USA.

Presented at Digestive Disease Week, May 21-24, Los Angeles, California (Gastrointest Endosc 2006;63:AB256), and Digestive Disease Week, May 20-23, 2007, Washington, DC (Gastrointest Endosc 2007;65:AB103).

Reprint requests: Ananya Das, MD, Division of Gastroenterology and Hepatology, Mayo Clinic Scottsdale, 13400 East Shea Blvd, Scottsdale, AZ 85259.